

# Geostrophic Adjustment of a Zero Potential Vorticity Flow Initiated by a Mass Imbalance

RONGSHENG WU

*Department of Atmospheric Sciences, Nanjing University, People's Republic of China*

WILLIAM BLUMEN

*Astrophysical, Planetary, and Atmospheric Sciences Department, University of Colorado, Boulder, Colorado*

15 December 1993 and 15 August 1994

## ABSTRACT

Geostrophic adjustment of fluid in constant rotation is considered. The initial state is characterized by a mass imbalance, the initial velocity field is geostrophic, and zero potential vorticity flow is imposed. The final balanced state is determined from conservation of potential vorticity (zero), linear momentum, and mass. The potential energy released during the adjustment process is partitioned into the kinetic and potential energies of the balanced state in the ratio 1:2, independent of the scale of the initial state. The development of a front (infinite relative vorticity and a zero-order discontinuity in density) does, however, depend on the spatial scales of the initial fields. Moreover, the initial position of the maximum vorticity relative to the initial position of the maximum density gradient significantly affects the balanced flow. Physical interpretations of the principal features are provided.

## 1. Introduction

Mass and/or momentum imbalances of fluid in rotation initiate an adaptation process to an ultimate state of geostrophic or gradient balance. This process, referred to as geostrophic adjustment, is continually operating in both the atmosphere and oceans. A momentum imbalance by an imposed wind stress on the ocean surface provided the earliest model of the adjustment process (Rossby 1937, 1938). A shelf-slope front provides an example of adaptation of the mass field (Ou 1984). In principle, the simple prototypical models that have been used to delineate the adjustment process are deficient because some sidestep the time-dependent process (Rossby and Ou's work are examples), while others linearize the problem [the work of Cahn (1945) and Obukhov (1949), for example, falls into this class]. These simple models do, however, provide physical insights and principles that may not be evident in the examination of the fully nonlinear adjustment process in stratified fluid. It is this prototypical approach that motivates the present note.

Ou (1984, 1986) analyzed the adjustment of an initial mass imbalance to a state of geostrophic balance and established two significant features: 1) A relatively large initial density gradient will lead to the development of a zero-order discontinuity in the final state

density distribution and, correspondingly, the relative vorticity of the geostrophic flow becomes infinite. 2) One-half of the potential energy released by the adaptation of the initial mass field is distributed to the balanced kinetic energy, while the other half is distributed to transient motions.

The present study extends Ou's analysis by specification of a balanced momentum field to accompany the mass imbalance in the initial state. This model is briefly reviewed in section 2. It is then shown, in section 3, that the initial momentum field does not release any kinetic energy in the adaptation to a final state of geostrophic balance. It is the initial mass imbalance that provides the potential energy source, and this released energy is distributed to the final kinetic and potential energies in the ratio 1:2, as in Ou (1986). Frontal formation is displayed as a nonlinear self-advection process in section 4, and various balanced flows that have evolved from specified initial states are displayed and interpreted in section 5. Although this study does expose some relatively simple basic principles that control adjustment of a zero potential vorticity flow, the extension of the model to describe the time-dependent adjustment process or the relaxation of the zero potential vorticity constraint has not been attempted.

## 2. Model and solution

The present model, introduced by Ou (1984), considers incompressible, inviscid flow in two dimensions ( $x, z$ ), where  $x$  is the horizontal and  $z$  the vertical coordinate. The fluid is in constant rotation at angular

*Corresponding author address:* Dr. William Blumen, Astrophysical, Planetary, and Atmospheric Sciences Department, University of Colorado, Campus Box 391, Boulder, CO 80309-0391.

velocity  $f/2$ , where  $f$  is the Coriolis parameter. Ou's model has been reexamined by Blumen and Wu (1995, hereafter BW). This model is described by three principles, presented as (1), (2), and (3) in BW: conservation of potential vorticity, linear momentum, and density. The first principle, displayed in (11) in BW, establishes that if the potential vorticity vanishes, then the density  $\rho$  is only a function of the momentum coordinate  $X = x + v/f$ , where  $v(x, z)$  is the velocity component normal to the  $x$  axis. The second principle requires

$$X = X_0 = x_0 + \frac{v_0(x_0)}{f}, \quad (1)$$

where the initial state, denoted by subscript 0, is independent of the vertical coordinate. The third principle reduces to

$$\rho(X) = \rho(X_0) \quad (2)$$

for zero potential vorticity flow. An initial mass imbalance, specified by  $\rho_0(x_0)$ , is imposed. The initial velocity is also depth independent and given by  $v_0(x_0)$ . This latter field must, however, be in geostrophic balance with the vertical average of the pressure gradient force. This balance is a consequence of the rigid lids imposed at the top and bottom boundaries (Williams 1967). A succinct presentation of the Williams proof appears in the appendix.

All variables may be cast into nondimensional form by means of

$$x = \lambda x', \quad z = h z', \quad v = (g^* h)^{1/2} v',$$

where  $h$  denotes the distance between two rigid surfaces,  $g^* = g \Delta \rho / \rho(0)$  denotes "reduced gravity,"  $\Delta \rho$  is the characteristic amplitude of the density anomaly, and  $\lambda = (g^* h)^{1/2} f^{-1}$  is the internal deformation radius. The prime notation will be omitted from the nondimensional quantities.

The following two additional constraints are introduced (see BW, section 2). The final state is determined directly from the initial state,  $\rho_0(x_0)$  and  $v_0(x_0)$ , using the conservation principles and, therefore, bypassing the transient adjustment process. Further, the final state is assumed to be a stationary state of geostrophic balance, and the final velocity  $v(x, z)$  is determined from  $v_0(x_0)$  and the state of thermal wind balance, expressed in momentum coordinates, as

$$\frac{\partial v}{\partial Z} = - \frac{\partial \rho}{\partial X}, \quad (3)$$

where  $z = Z$  and  $\rho$  is found from (2).

The solutions for  $\rho(x, z)$  and  $v(x, z)$ , when there is an initial mass imbalance  $\rho_0(x_0)$  but an initial geostrophically balanced flow  $v_0(x_0)$ , may be derived as in BW, where the case  $v_0(x_0) = 0$  is examined. Since  $\rho = \rho(X)$ , the cross-stream velocity may be obtained from (3) and represented as

$$v = - \frac{d\rho}{dX} Z + g(X), \quad (4)$$

where  $g(X)$  is to be determined. Use of (1) and (2) casts (4) into the form

$$x_0 - x = -v_0 - \frac{d\rho_0}{dX_0} Z + g(X_0). \quad (5)$$

The displacement of isopycnal surfaces,  $x_0 - x$ , varies linearly with  $Z = z$ . This displacement is chosen to be symmetric about midlevel  $Z = 1/2$ . The arbitrary function  $g$  is determined and the final state is

$$\left. \begin{aligned} v &= v_0(X_0) + \frac{d\rho_0}{dX_0} \left( \frac{1}{2} - Z \right) \\ \rho &= \rho_0(X_0) \end{aligned} \right\}. \quad (6)$$

Although the only apparent difference between (6) and the simpler solution (14) in BW is the presence of  $v_0(X_0)$ , the two solutions can be quite dissimilar. The reason is that the position  $x$  of isopycnals and isovels of velocity are determined by

$$x = X_0 - v, \quad (7)$$

where  $X_0$  is given by (1) and  $v$  by (6).

### 3. Energy change

The kinetic and potential energies change by amounts

$$\Delta \text{KE} = \frac{1}{2} \int_{-\infty}^{\infty} \int_0^1 v^2 dz dx - \frac{1}{2} \int_{-\infty}^{\infty} \int_0^1 v_0^2 dz_0 dx_0 \quad (8)$$

and

$$\Delta \text{PE} = \int_{-\infty}^{\infty} \int_0^1 \rho_0 z_0 dz_0 dx_0 - \int_{-\infty}^{\infty} \int_0^1 \rho z dz dx \quad (9)$$

during the adjustment process. Ou (1986) showed that  $\gamma = \Delta \text{KE} / \Delta \text{PE} = 1/2$ , independent of the initial scale of  $\rho_0(x_0)$ . Ou's result, valid for  $v_0(x_0) = 0$ , will be extended to include an initially balanced flow  $v_0(x_0)$ . The method will be that of BW.

The change in potential energy is presented in BW by (22). The same development may be followed but here mass conservation and the coordinate transformation, provided by (6) and (7), recasts (9) as

$$\Delta \text{PE} = \frac{1}{12} \int_{-\infty}^{\infty} \left( \frac{\partial \rho_0}{\partial X_0} \right)^2 dX_0. \quad (10)$$

The change in kinetic energy can also be determined as in BW, but the initial kinetic energy must be included in the derivation. Consider the final state ( $f$ ) and introduce momentum coordinates to obtain

$$\begin{aligned}
 K_f &= \frac{1}{2} \int_{-\infty}^{\infty} \int_0^1 v^2 dx dz \\
 &= \frac{1}{2} \int_0^1 \int_{-\infty}^{\infty} v^2 \left(1 - \frac{\partial v}{\partial X}\right) dX dZ \\
 &= \frac{1}{2} \int_0^1 \int_{-\infty}^{\infty} v^2 dX dZ, \tag{11}
 \end{aligned}$$

where  $v \rightarrow 0$  as  $X \rightarrow x \rightarrow \infty$ . Now (6) may be inserted into (11) to obtain

$$\begin{aligned}
 K_f &= \frac{1}{2} \int_{-\infty}^{\infty} \int_0^1 \left(\frac{d\rho_0}{dX_0}\right)^2 \left(\frac{1}{2} - Z\right)^2 dZ dX_0 \\
 &\quad + \int_{-\infty}^{\infty} \int_0^1 v_0(X_0)^2 dZ dX_0, \tag{12}
 \end{aligned}$$

where  $dX = dX_0$  and the cross-product term drops out upon integration over  $Z$ . The last term in (12) is  $K_i$ , the initial kinetic energy, which may be verified by use of  $dx_0 = (1 - \partial v_0/\partial X_0)dX_0$  and integration as in (11). Finally, (12) may be expressed as

$$K_f = K_i + \frac{1}{24} \int_{-\infty}^{\infty} \left(\frac{d\rho_0}{dX_0}\right)^2 dX_0 \tag{13}$$

following integration with respect to  $Z$ . There is a concomitant increase of kinetic energy with a loss of initial potential energy. Moreover, this latter energy source is partitioned according to (10) and (13) in the ratio  $|\gamma| = 1/2$ , as in the case when  $v_0 = 0$ .

#### 4. Frontal formation

The condition for frontal formation may be determined from the Jacobian of the transformation from  $(x, z)$  to  $(X, Z)$  space (Hoskins 1975):

$$1 + \frac{\partial v}{\partial x} = \left(1 - \frac{\partial v}{\partial X}\right)^{-1}. \tag{14}$$

In the present context, a front occurs at the point, on a rigid boundary where  $\partial v/\partial x = \infty$ , or where  $\partial v/\partial X = 1$ . Condition (14), together with (6), may be used to confirm Ou's (1984) result that frontal formation occurs simultaneously at the upper and lower surfaces when  $|\partial^2 \rho_0/\partial x_0^2| = 2$ , with  $\rho_0$  specified by (18).

An alternate, and perhaps a more physically motivated, derivation of the condition for a front to form may be established. It is based on the observation that if  $v = f(x + vt)$ , where  $f$  is some function of the variable  $x + vt$  and  $t$  is time, then

$$\frac{\partial v}{\partial t} - v \frac{\partial v}{\partial x} = 0. \tag{15}$$

Equation (15) is a nonlinear advection equation that produces a result  $\partial v/\partial x = \infty$  in a finite time  $t_c$  (e.g., Lighthill 1978). This critical time may be determined by differentiating (15) to obtain

$$\frac{d}{dt} \left(\frac{\partial v}{\partial x}\right)^{-1} = -1, \tag{16}$$

where  $d/dt$  denotes differentiation in a coordinate system following the motion. Integration from the initial to final state, when  $\partial v/\partial x = \infty$ , yields

$$t_c = \left(\frac{\partial v_0}{\partial x_0} \Big|_{\max}\right)^{-1}. \tag{17}$$

The situation leading to (17) presents itself here. Consider the case  $v_0(x_0) = 0$ , so that (1) reduces to  $X_0 = x_0$ . The initial density will be represented by

$$\rho_0 = \epsilon \tanh \beta x_0, \tag{18}$$

where  $(\epsilon, \beta^{-1})$  denote, respectively, amplitude and length scale. Then (6) becomes

$$\begin{aligned}
 v &= \left(\frac{1}{2} - z\right) \epsilon \beta \operatorname{sech}^2 \beta x_0 \\
 &= \left(\frac{1}{2} - z\right) \epsilon \beta \operatorname{sech}^2 \beta(x + v), \tag{19}
 \end{aligned}$$

if use is made of the momentum coordinate. Now (19) has the form that is appropriate to derive an "advection equation." It is, however, necessary to define the appropriate parameter to replace  $t$ . Consider the solution at the lower boundary,  $z = 0$ , and define  $\chi = \beta x$ ,  $V = v(\epsilon\beta/2)^{-1}$ , and  $\tau = \epsilon\beta^2/2$ . Then  $V$  satisfies

$$\frac{\partial V}{\partial \tau} - V \frac{\partial V}{\partial \chi} = 0, \tag{20}$$

and

$$\tau_c = \left(\frac{\partial V_0}{\partial \chi_0}\right)^{-1}_{\max}. \tag{21}$$

The critical value of  $\tau_c$  depends on the initial amplitude, the initial scale, or both. If, for example, the amplitude is fixed, then the initial density gradient must be sufficiently large for frontal formation to occur. The determination of  $\tau_c$ , or equivalently  $\beta_c$ , by (21) is equivalent to its determination by use of (14). For example, if  $\epsilon = 1/2$ , then  $\beta_c = 2.28$ .<sup>1</sup>

The identical consideration may be applied to (6) when  $v_0 \neq 0$ , for then use of  $X_0 = X = x + v$  casts  $v$  into the form  $v = f(x + v)$ . The actual determination of a critical parameter to establish frontal formation will, in general, require a numerical effort if the number of parameters is increased by the addition of  $v_0$ .

#### 5. Examples and interpretation

The initial state is assumed to be the mass imbalance (18) imposed by Ou (1984) and a geostrophic momentum field provided by

<sup>1</sup> Ou's numerical value  $\beta_c = 2.6$  is in error.

$$v_0 = \frac{1}{2} \operatorname{sech}^2 \alpha x_0, \quad (22)$$

where  $\alpha^{-1}$  is the length scale of this velocity jet. It is difficult to find observational evidence of a characteristic state to model an oceanic or atmospheric imbalance that would fit the present constraints. The present intent is to demonstrate the principle of adaptation to a geostrophically balanced flow rather than to provide a detailed description of a particular phenomenon. Some flexibility will, however, be introduced by representing the mass imbalance by

$$\rho_0 = \pm \frac{1}{2} \tanh(\beta x_0 + \phi), \quad (23)$$

where  $\phi$  denotes a constant displacement. In this representation the maximum relative vorticity may be displaced from the maximum density gradient, and the spatial scales of the velocity and density distributions may differ.

Frontal formation is determined by fixing two of the three parameters ( $\alpha, \beta, \phi$ ) and then finding the critical value of the third parameter by numerical evaluation of  $1 - \partial v / \partial X = 0$ . This straightforward evaluation makes use of (6) and the relation

$$\frac{\partial}{\partial X} = \frac{\partial}{\partial X_0} = \left(1 + \frac{\partial v_0}{\partial x_0}\right)^{-1} \frac{\partial}{\partial x_0}. \quad (24)$$

The equivalent condition for frontal formation is

$$\left| \frac{\partial}{\partial x_0} \left( \frac{\partial \rho_0 / \partial x_0}{1 + \partial v_0 / \partial x_0} \right) \right| = 2, \quad (25)$$

which reduces to Ou's (1984) condition when  $v_0 = 0$ . Further evaluation proceeds from (6), (22), and (23).

Two representations are considered:

- 1)  $\alpha = 1, \quad -\pi/4 \leq \phi \leq \pi/4$
- 2)  $\beta = 1, \quad -\pi/4 \leq \phi \leq \pi/4$ .

The sign of  $\rho_0$  in (23) is chosen to produce a front at  $z = 0$  rather than at  $z = 1$ . Numerical evaluation of  $\beta_c$  was carried out for 11 values of  $\phi$ , and 10 values were used to find  $\alpha_c$ .

The significant physical aspects of all 21 cases are essentially contained in three cases: namely,

- $\alpha = 1, \quad \phi = 0, \quad \beta_c = 2.219,$
- $\beta = 1, \quad \phi = 0, \quad \alpha_c = 1.554,$
- $\beta = 1, \quad \phi = \pi/4, \quad \alpha_c = 1.901.$

These cases will also be compared with Ou's example:  $v_0 = 0$  and  $\beta = 2.283$ , displayed in Fig. 1.

The distinguishing feature of Fig. 1 is frontal formation at both top and bottom, and the presence of boundary jet flows behind each of the frontal positions. The geostrophic velocity  $v$  for this case satisfies thermal wind balance, and its axis slopes linearly with height;

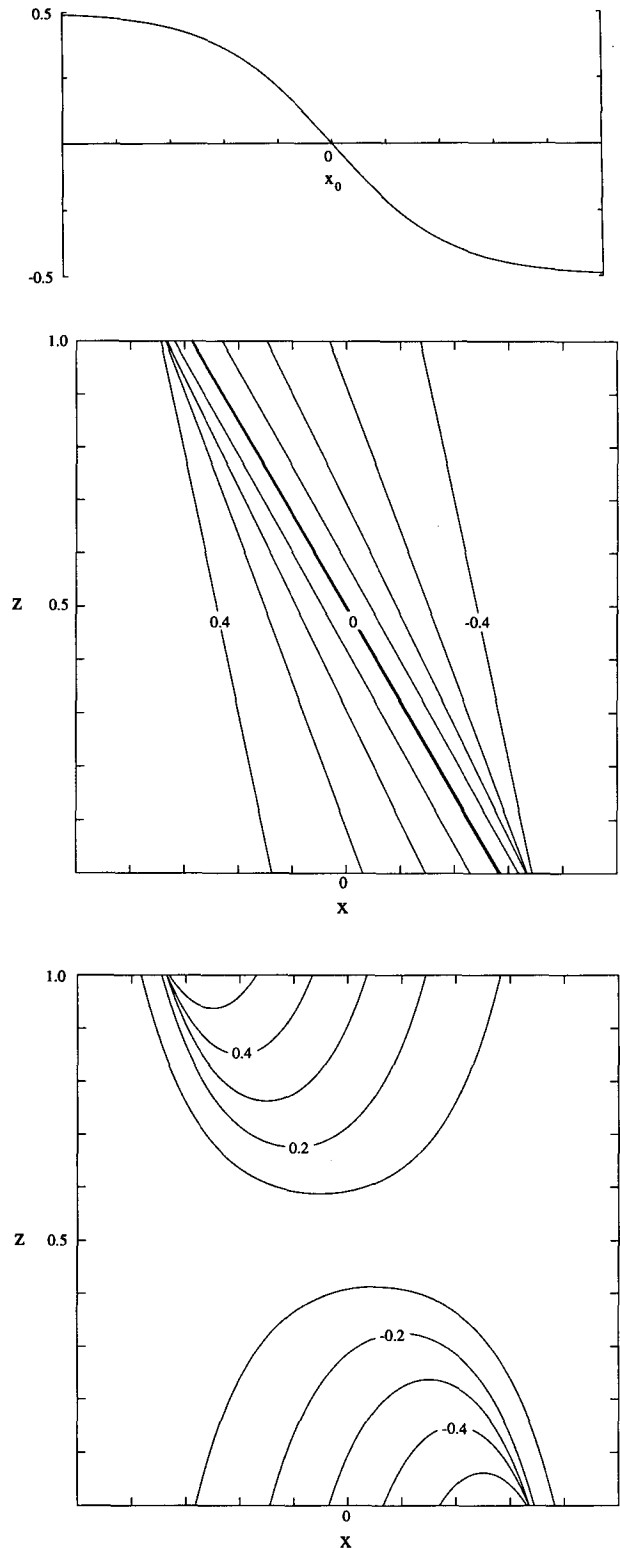


FIG. 1. Initial density distribution as a function of  $x_0$  with  $v_0 = 0$  (top). Final density distribution, represented by isopycnals in the  $(x, z)$  plane (middle), with  $\beta_c = 2.283$ . Geostrophic velocity distribution in the final state (bottom). All variables are nondimensional with  $\Delta z = 0.1$  and  $\Delta x = 0.2$ .

the zero-order discontinuities in  $(\rho, v)$  coincide at both boundaries. The added presence of a barotropic geostrophic flow  $v_0$ , exhibited by (6), introduces an asymmetry in both the density and the flow field that is evident in Figs. 2–4. The case presented in Fig. 2 displays a front at  $z = 0$ , but not at  $z = 1$  (a front forms at both boundaries when  $\phi = 0.038$ ). The velocity jets exhibit vertical asymmetry with the lower jet more confined to the lower boundary. This case may be contrasted with Fig. 3, where a front is also present at the lower boundary (a front forms at both boundaries when  $\phi = -0.079$ ). Deep penetration into the interior by the lower jet flow is the most prominent feature of this case.

In all cases, the initial unbalanced density distribution simply pivots about midlevel to attain a stable frontal orientation, which releases potential energy and establishes a thermal wind balance. The distinctive features that arise, in comparison with Fig. 1, are associated with two properties of the initial state: 1) the relative difference in the spatial scales of  $v_0$  and  $\rho_0$ , and 2) the position of the maximum positive vorticity relative to the position of the maximum density gradient. These properties are both reflected in the condition that determines frontal formation (25).

Frontal formation occurs where the relative vorticity is positive. The contribution is made up from a barotropic part  $v_0$ , expressed by (22), and a baroclinic part associated with the horizontal gradient of  $\rho_0$ . The baroclinic contribution in Fig. 2 is similar to that in Fig. 1: the surface velocity is negative at the front, but its vorticity is positive. This latter feature is necessary to produce frontal formation, because the barotropic part of the flow exhibits negative vorticity at the frontal position. The sign of the velocity  $v$  is, however, positive, and because the baroclinic shear is positive, the geostrophic flow increases monotonically with height. Figure 3 presents a situation where the barotropic and the baroclinic flows are positive, and both exhibit positive relative vorticity at the frontal position. The relatively large geostrophic velocity  $v$  does, however, decrease with height because the baroclinic shear is negative. As indicated above, it is possible to adjust the relative phases and scales of the two fields to achieve either simultaneous frontal formation at the top boundary or only frontal formation at this boundary.

The final case, distinguished by  $\beta = 1$ ,  $\phi = \pi/4$ , and  $\alpha_c = 1.901$ , is displayed in Fig. 4. It exhibits a relatively confined surface jet at the frontal position as in Fig. 2 for the reason discussed above. There is, however, a secondary prominent positive vorticity axis deep into the relatively dense fluid. This feature is located where the barotropic and baroclinic flows both exhibit positive relative vorticity, as indicated by the vertical slope of the vorticity axis.

All the other cases can be interpreted using the principles applied to Figs. 1–4.

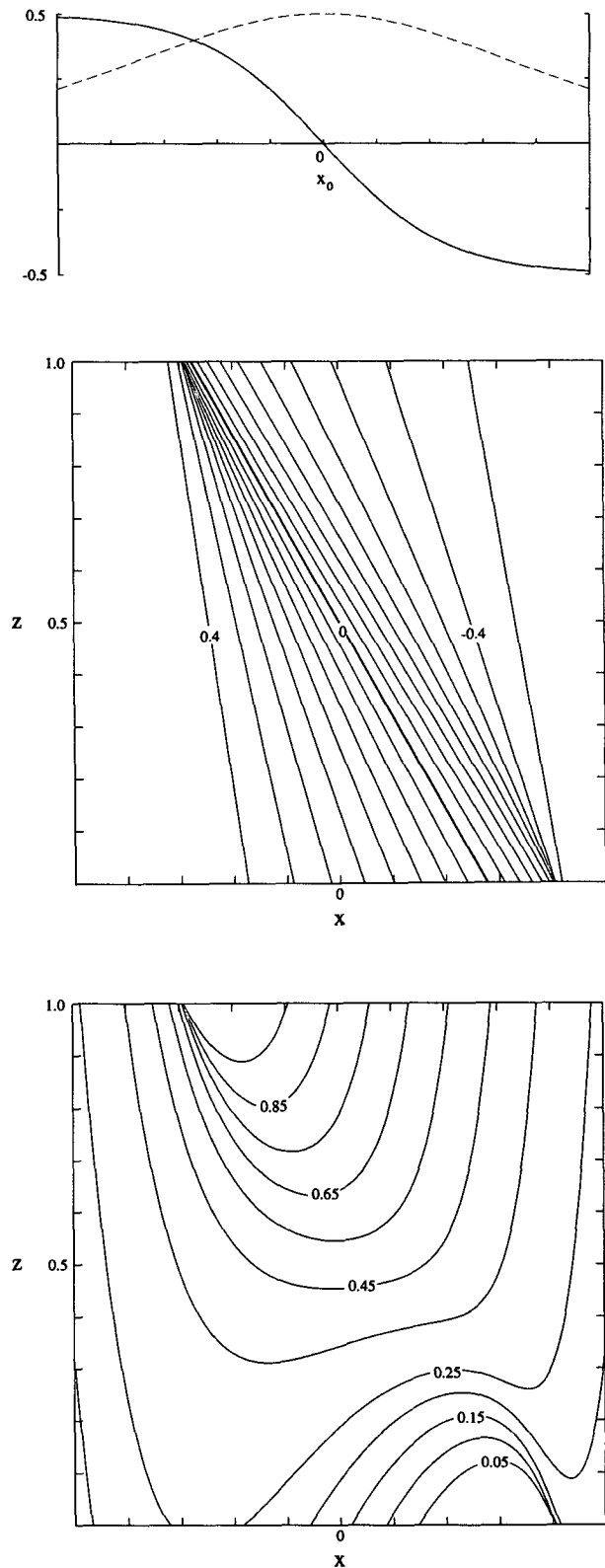


FIG. 2. As in Fig. 1 except the initial velocity  $v_0(x_0)$  appears as a dashed line in the top panel, and  $\alpha = 1$ ,  $\phi = 0$ , and  $\beta_c = 2.219$ . The gradient of  $v$  is enhanced in the lower part of the bottom panel.

6. Final remarks

Ou's (1984, 1986) geostrophic adjustment model has been extended to include an initial geostrophic velocity  $v_0$ , but zero potential vorticity flow is maintained.

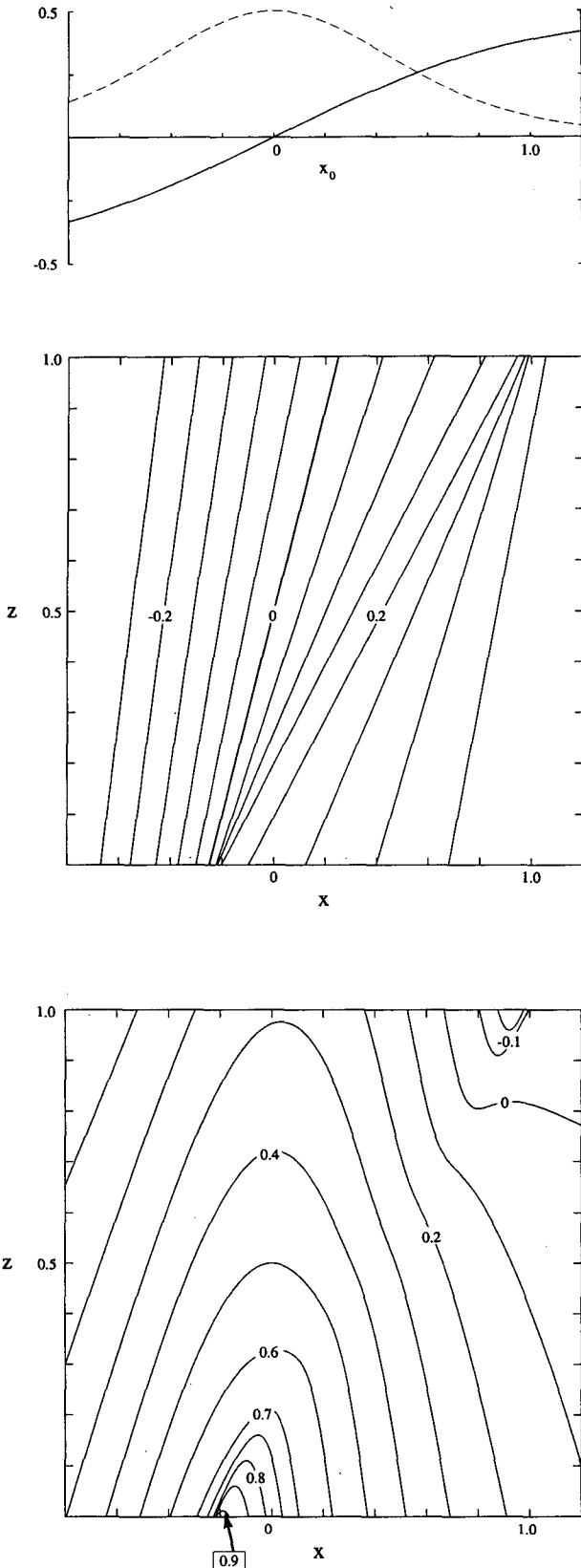


FIG. 3. As in Fig. 2 except  $\beta = 1$ ,  $\phi = 0$ , and  $\alpha_c = 1.554$ .

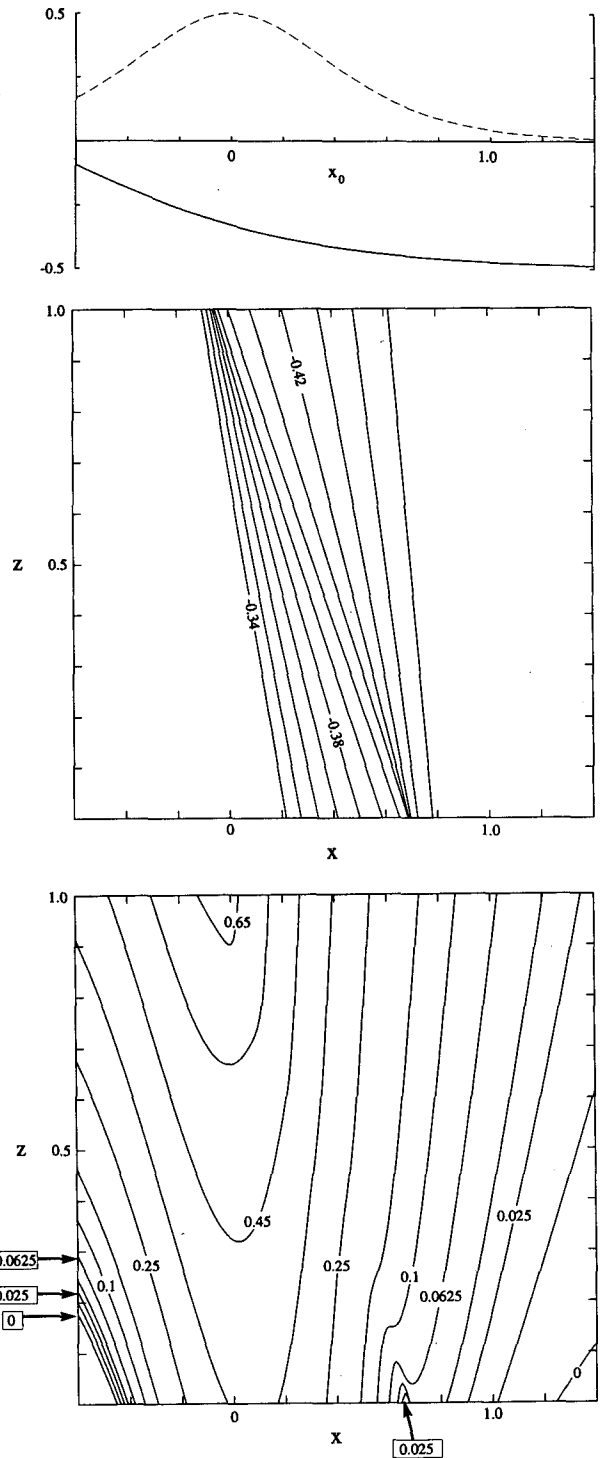


FIG. 4. As in Fig. 2 except  $\beta = 1$ ,  $\phi = \pi/4$ , and  $\alpha_c = 1.901$ .

Under this latter constraint none of the initial kinetic energy is available to reestablish a balanced geostrophic flow: the initial mass imbalance provides the necessary energy source for partition into the balanced state. As a consequence, the energy conversion ratio  $\Delta KE/\Delta PE = 1/2$  is the same value formed by Ou (1986) when  $v_0 = 0$ . This feature is clearly a limitation of the model and would not characterize uniform or nonuniform potential vorticity flows.

The presence of  $v_0 \neq 0$ , however, produces a non-trivial modification of the final state. The scale of the velocity field may differ from the scale of the initial density field, and their maximum gradients may be displaced relative to each other. These characteristics of the initial state determine the position of frontal formation and introduce vertical asymmetries into the final density and velocity distributions that are examined in section 5. The extent to which these features would emerge in a less constrained fluid model has not been examined.

*Acknowledgments.* Financial support for this investigation has been provided by the National Science Foundation under Grants INT-9113566 and ATM-9303111. RW also acknowledges support by the National Natural Science Foundation of China and Nanjing University. We express our appreciation to Professor R. T. Williams for leading us to his 1967 paper.

#### APPENDIX

##### Initial Velocity Field

Consider the continuity equation

$$\frac{\partial u}{\partial x} + \frac{\partial w}{\partial z} = 0, \quad (\text{A1})$$

where  $(u, w)$  denote  $(x, z)$  velocity components. The vertical average over the fluid depth is denoted by a

bar, and  $w = 0$  at  $z = 0, h$ . The vertical average of (A1) establishes that  $\bar{u}_x = 0$ . Further, use of (A1) provides the flux form of the  $x$ -momentum equation

$$\frac{\partial u}{\partial t} + \frac{\partial}{\partial x} u^2 + \frac{\partial}{\partial z} uw - fv = -fv_g, \quad (\text{A2})$$

where  $t$  is time and  $v_g$ , the geostrophic velocity, is used to represent the pressure gradient force. Differentiation and a vertical average of (A2) provides a balance condition,

$$\frac{\partial}{\partial x} \left[ \frac{\partial}{\partial x} \bar{u}^2 + \frac{\partial}{\partial z} \bar{u}\bar{w} - f(\bar{v} - \bar{v}_g) \right] = 0, \quad (\text{A3})$$

satisfied by the flow field at any time  $t$ . In the present context, the initial conditions are  $u = w = 0$  and  $|v_0| = 0$  at  $|x_0| = \infty$ . Then (A3) establishes that an initial barotropic flow  $v_0(x_0)$  must be in geostrophic balance, with the vertical average of the pressure gradient force.

#### REFERENCES

- Blumen, W., and R. Wu, 1995: Geostrophic adjustment: Frontogenesis and energy conversion. *J. Phys. Oceanogr.*, **25**, 428–438.
- Cahn, A., 1945: An investigation of the free oscillations of a simple current-system. *J. Meteor.*, **2**, 113–119.
- Hoskins, B. J., 1975: The geostrophic momentum approximation and the semi-geostrophic equations. *J. Atmos. Sci.*, **3**, 233–242.
- Lighthill, J., 1978: *Waves in Fluids*. Cambridge University Press, 504 pp.
- Obukhov, A. M., 1949: On the question of the geostrophic wind. *Izv. Akad. Nauk SSSR Ser. Geograf-Geofiz.*, **13**, 281–306.
- Ou, H. W., 1984: Geostrophic adjustment: A mechanism for frontogenesis. *J. Phys. Oceanogr.*, **14**, 994–1000.
- , 1986: On the energy conversion during geostrophic adjustment. *J. Phys. Oceanogr.*, **16**, 2203–2204.
- Rosby, C.-G., 1937: On the mutual adjustment of pressure and velocity distribution in simple current systems, 1. *J. Mar. Res.*, **1**, 15–28.
- , 1938: On the mutual adjustment of pressure and velocity distribution in simple current systems, 2. *J. Mar. Res.*, **1**, 239–263.
- Williams, R. T., 1967: Atmospheric frontogenesis: Numerical experiment. *J. Atmos. Sci.*, **24**, 627–641.